

Validation of Shadowgraph Spectral Analysis using an SLS Block 2 Wind-Tunnel Model

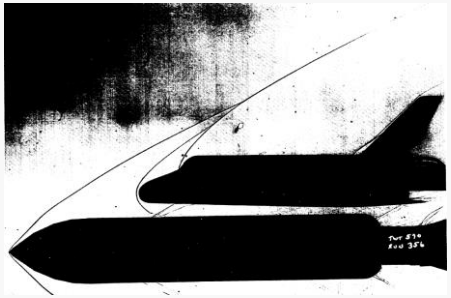
AIAA SciTech
23–27 January 2023
National Harbor, MD & Online

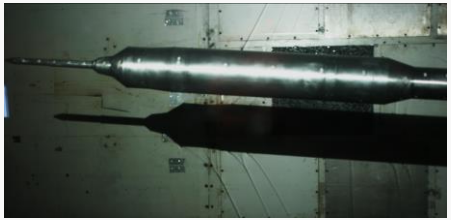
Oleg Goushcha and Martin K. Sekula
NASA Langley Research Center, Hampton, VA 23681
Theodore J. Garbeff II
NASA Ames Research Center, Moffett Field, CA, 94035

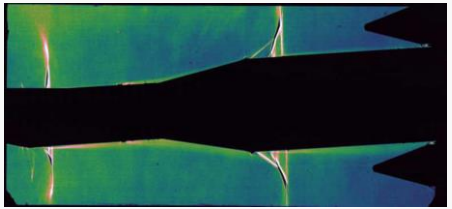
Copyright 2023 United States Government as represented by the Administrator of the National Aeronautics and Space Administration. No copyright is claimed in the United States under Title 17, U.S. Code. All Other Rights Reserved. Published by the American Institute of Aeronautics and Astronautics, Inc. with permission.

Introduction: shadowgraph

- **A shadowgraph is a method used to visualize the flow and is often used to supplement and explain direct flow property measurements**
- **Implementation seen in:**
  - Space Shuttle (STS) program[1]
  - Constellation (Ares I-X) program[2]
  - Space Launch System (SLS) program[3]







[1]Springer, A., "Shadowgraph Study of Space Transportation System (STS): The Space Shuttle Launch Vehicle (SSLV)", 1994.
[2]PiatakA D. J., Sekula, M. K., and Rausch, R. D., "Comparison of Ares I-X Wind-Tunnel-Derived Buffet Environment with Flight Data," *Journal of Spacecraft and Rockets*, Vol. 49, No. 5, 2012, pp. 822–833. https://doi.org/10.2514/1.A32176.
[3]Heaney, P. S., Soranna, F., Sekula, M. K., Piatak, D. J., and Ramey, J. M., "Analysis of Transonic Unsteady Aerodynamic Environments using Unsteady Pressure Sensitive Paint for the Space Launch System Block 1 Cargo Launch Vehicle," *AIAA SciTech 2021 Forum*, Virtual, 2021.

Introduction: objective

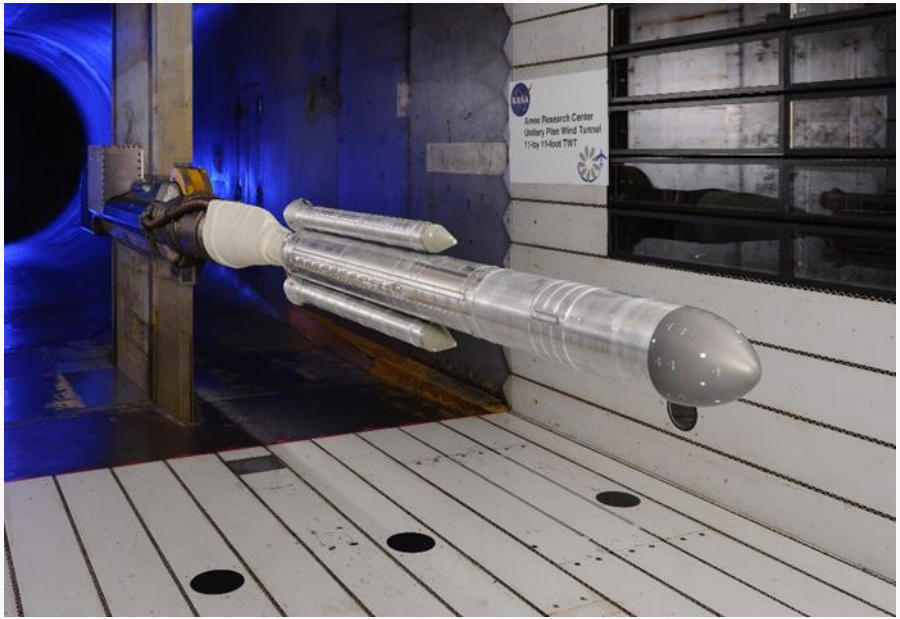
- **Develop a technique to extract pressure measurements from shadowgraph videos**

- **Previously the quantitative shadowgraph flow visualization has been seen in:**
  - Medical field to develop ultrasound techniques[4]
  - Flow properties of the supersonic free-jets[5]
  - Cavitation flows in fuel injection nozzles[6]

[4]Miyasaka, R., Harigane, S., Yoshizawa, S., and Umemura, S., "Quantitative Measurement of Highly Focused Ultrasound Pressure Field by Optical Shadowgraph," *Journal of Physics: Conference Series*, Vol. 520, No. 1, 2014, p. 012026.
[5] Koponen, E., Leskinen, J., Tarvainen, T., and Pulkkinen, A., "Acoustic pressure field estimation methods for synthetic schlieren tomography," *The Journal of the Acoustical Society of America*, Vol. 145, No. 4, 2019, pp. 2470–2479.
[6]Kolhe, P., Ivanchenko, O., Agrawal, A., and Olcmen, S., "Experimental Measurement of Density, Pressure and Temperature Fields in a Supersonic Free Jet Using Rainbow Schlieren Deflectometry," *46th AIAA Aerospace Sciences Meeting and Exhibit*, 2008.

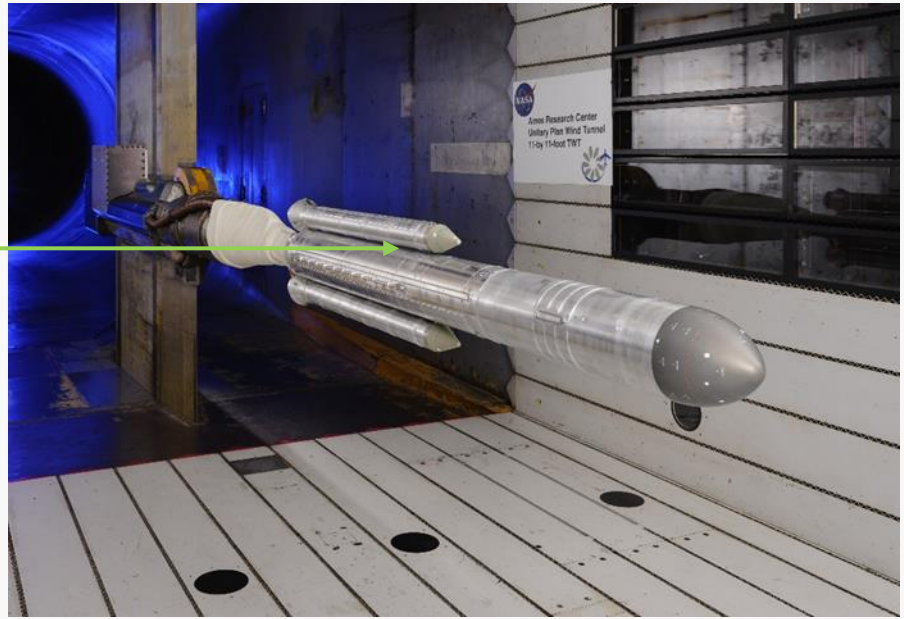
Experimental setup: wind-tunnel test

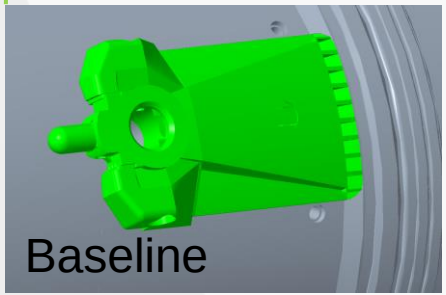
- Using data from the Booster Obsolescence Life Extension (BOLE) Forward Attachment Structure Trade Study Test (BFASTST)
- Performed at the NASA Ames Research Center Unitary 11- by 11-Foot Transonic Wind Tunnel
- 2.5 percent model of the SLS Block 2 Cargo vehicle

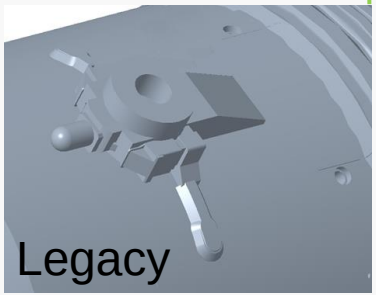


Experimental setup: model configurations

- Primary objective of the test was to investigate the aerodynamic environment downstream of various booster forward attachment hardware geometries
- In total, seven geometries were studied during test
- Only two will be used in the present discussion:

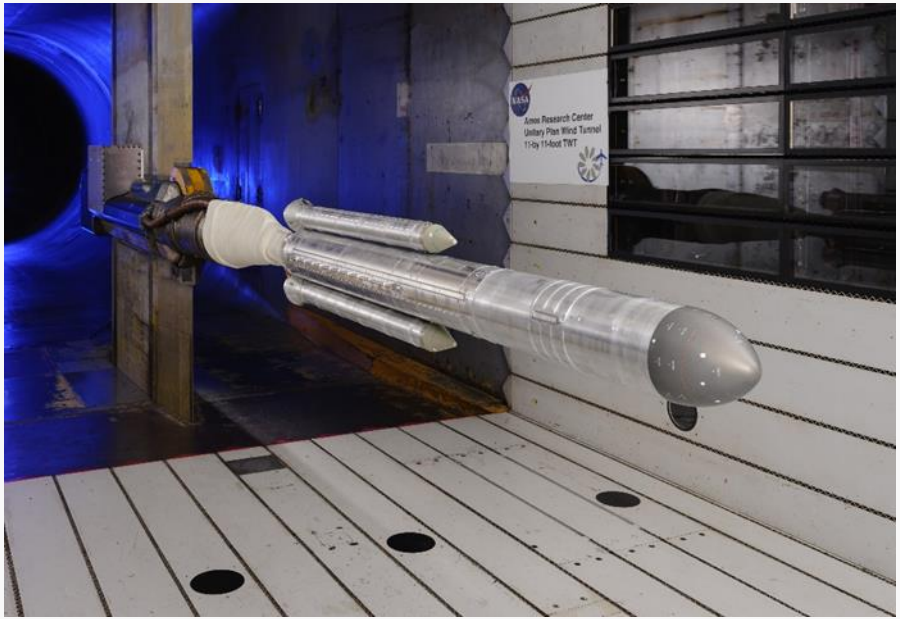






Experimental setup: instrumentation

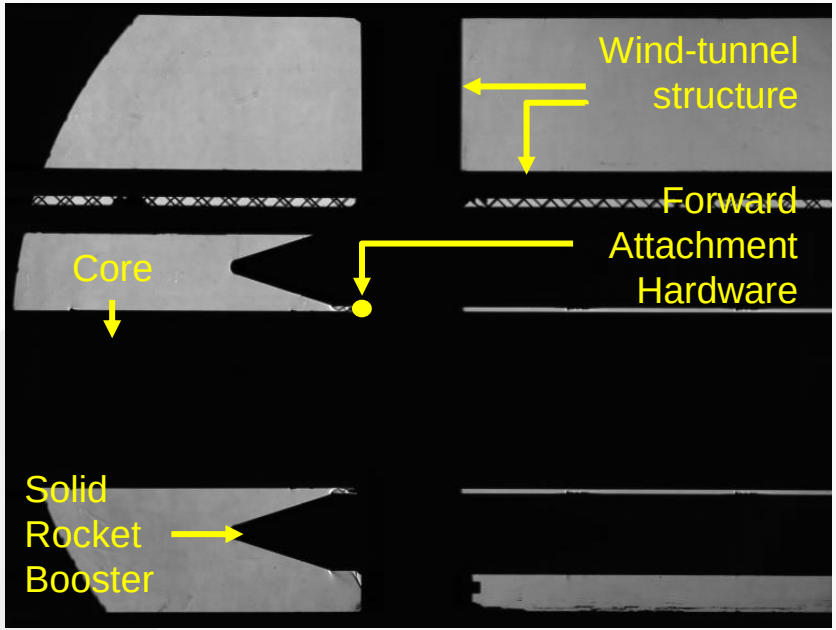
- Pressure measurements:
  - 189 Kulite® pressure transducers
  - "Slow" record: 10,000 Hz for 15 s
  - "Fast" record: 200,000 Hz for 2 s
- Shadowgraph:
  - Phantom v2511 series high-speed camera
  - Production-level setup[7]
  - 51,000 Hz rate
- Flow conditions:
  - Mach number ranged from 0.60 to 1.20
  - Attitude was varied in pitch and sideslip from -6° to 6°

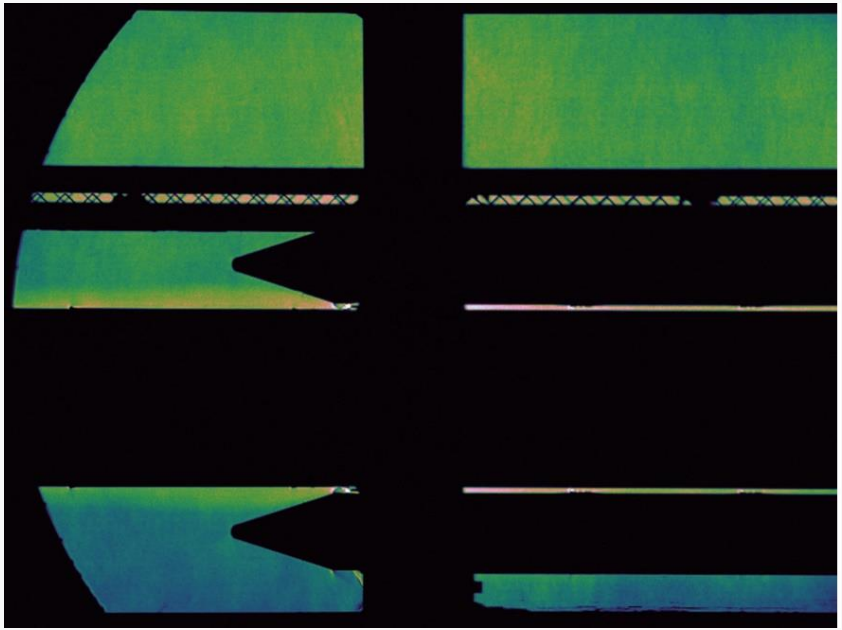


[7]Garbeff, T. J., Baerny, J., and Ross, J. C., "Wind Tunnel Flow Field Visualizations of the Space Launch System Vehicle Ascent,"

Experimental setup: shadowgraph view

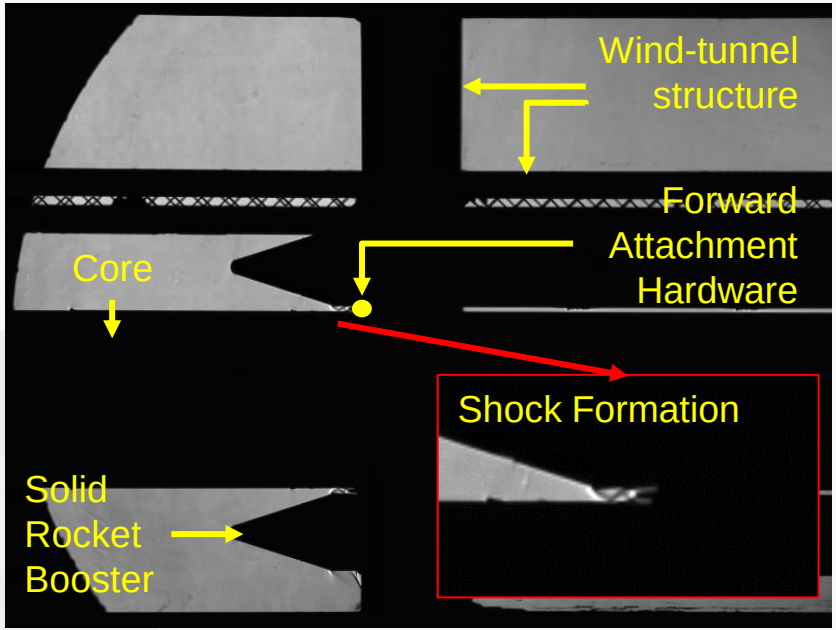
- Representative shadowgraph images obtained at $M = 0.92, \beta = 0°$
- Ensemble-averaged image and standard deviation image

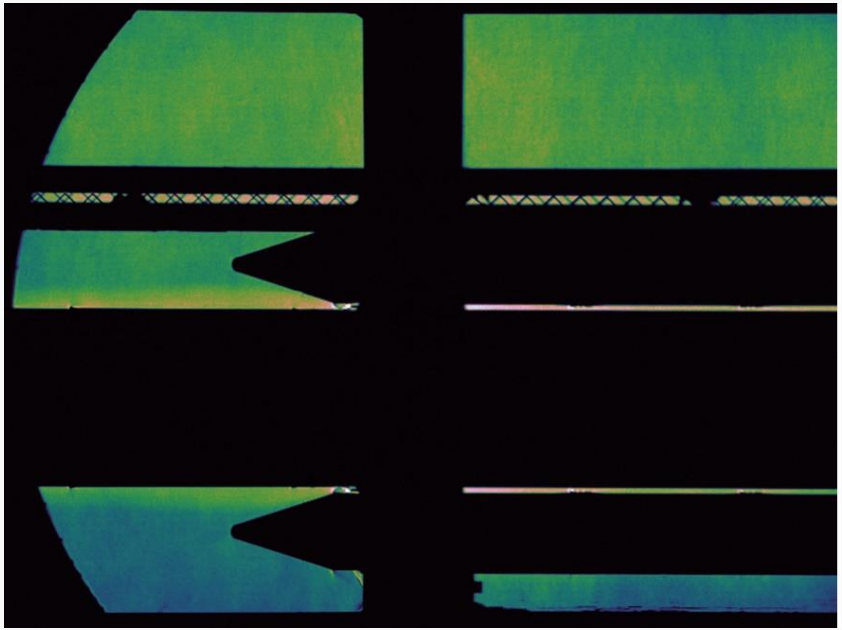




Experimental setup: shadowgraph view

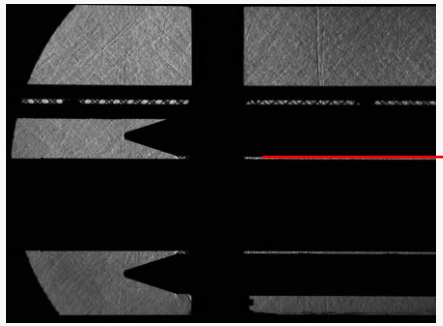
- Representative shadowgraph images obtained at $M = 0.92, \beta = 0°$
- Ensemble-averaged image and standard deviation image



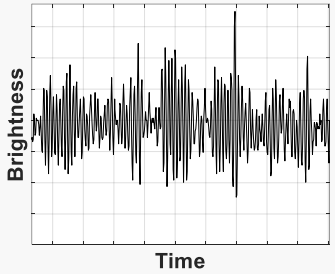


Analysis: FFT of shadowgraph

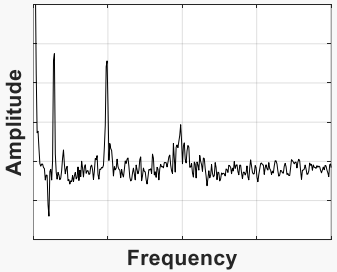
- Analysis begins by **extracting a time-series of the light intensity,** I, from a shadowgraph video for each pixel
- **Discrete Fast Fourier Transform (FFT)** analysis was performed on each time-series
- For each frequency, the **FFT amplitudes of all pixels in the frame were averaged** to produce an ensemble FFT amplitude



Extract pixel brightness time-series



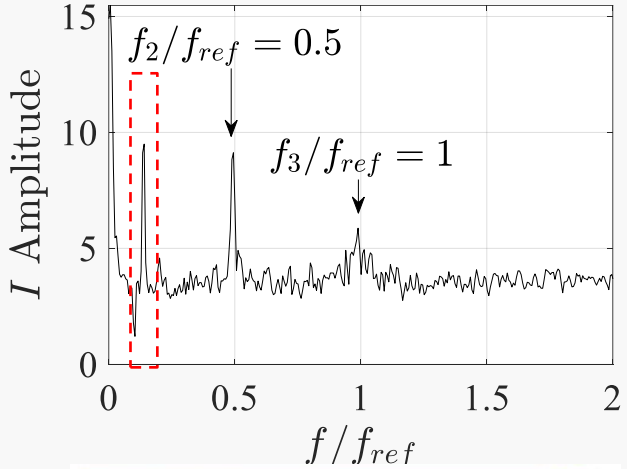
Perform FFT analysis

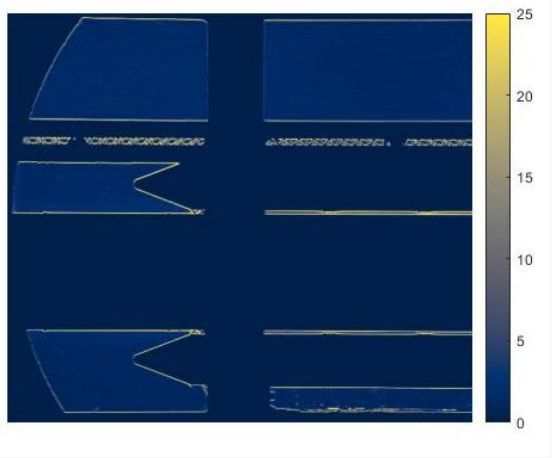


Ensemble average of all pixels in region of interest

Analysis: shadowgraph peaks

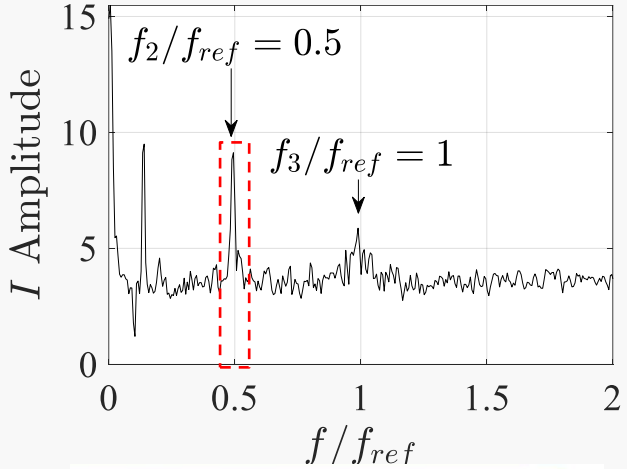
- All frequencies were normalized by f_3, which was used as the reference frequency f_{ref}
- Examining three dominant amplitude peaks:
  - f_1 likely corresponds to model and camera vibration

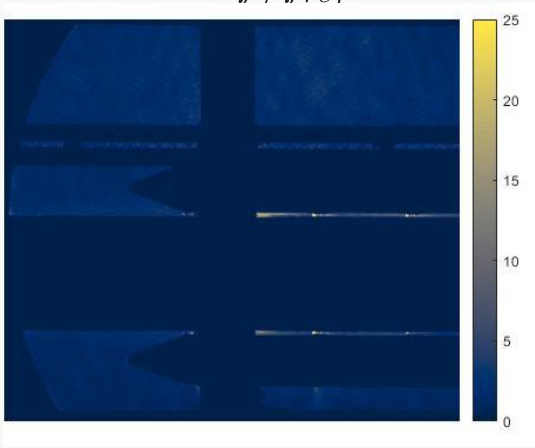




Analysis: shadowgraph peaks

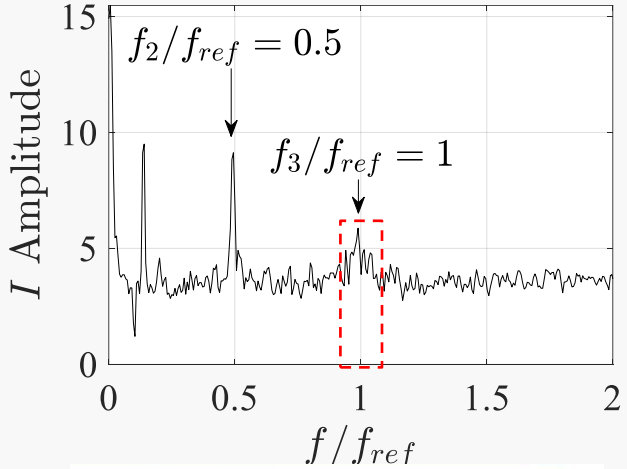
- All frequencies were normalized by f_3 which was used as reference frequency f_{ref}
- Examining three dominant amplitude peaks:
  - f_1 likely corresponds to model and camera vibration
  - f_2 fluctuations in flow downstream of the forward attachment hardware

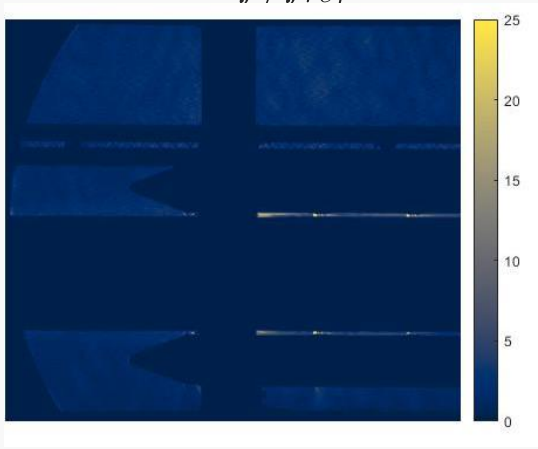




Analysis: shadowgraph peaks

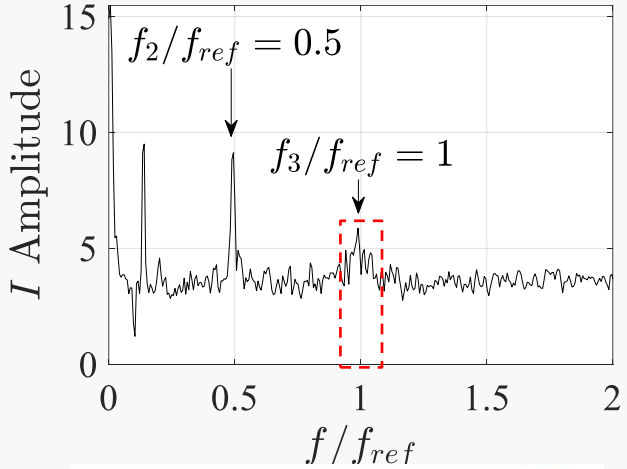
- All frequencies were normalized by f_3 which was used as reference frequency f_{ref}
- Examining three dominant amplitude peaks:
  - f_1 likely corresponds to model and camera vibration
  - f_2 fluctuations in flow downstream of the forward attachment hardware
  - f_3 fluctuations in flow downstream of the forward attachment hardware, harmonic of f_2

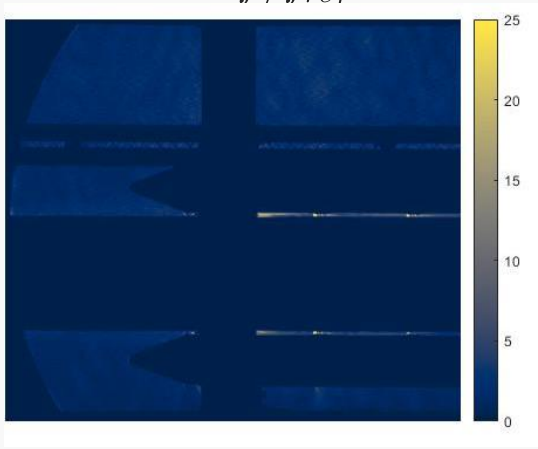




Analysis: shadowgraph peaks

- All frequencies were normalized by f_3 which was used as reference frequency f_{ref}
- Examining three dominant amplitude peaks:
  - f_1 likely corresponds to model and camera vibration
  - f_2 fluctuations in flow downstream of the forward attachment hardware
  - f_3 fluctuations in flow downstream of the forward attachment hardware, harmonic of f_2
- Dominant fluctuations in the flow field occur downstream of the forward attachment region
- **How can we relate amplitudes of I at f_2 and f_3 to pressure fluctuations?**



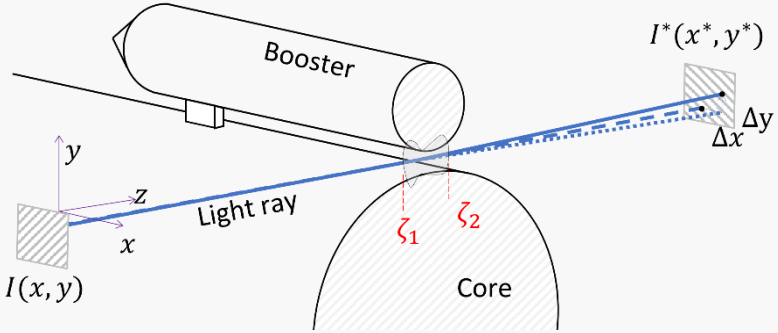


Analytical Considerations: governing equation

- Relation governing the change in image brightness intensity, I, as a function of, index of refraction, n:

$$\frac{\Delta I}{I} = l \int_{\zeta_1}^{\zeta_2} \left(\frac{\partial^2}{\partial x^2} + \frac{\partial^2}{\partial y^2} \right) (\ln n) dz$$

- A more detailed derivation is available in the manuscript, following Panigrahi et al.[8]

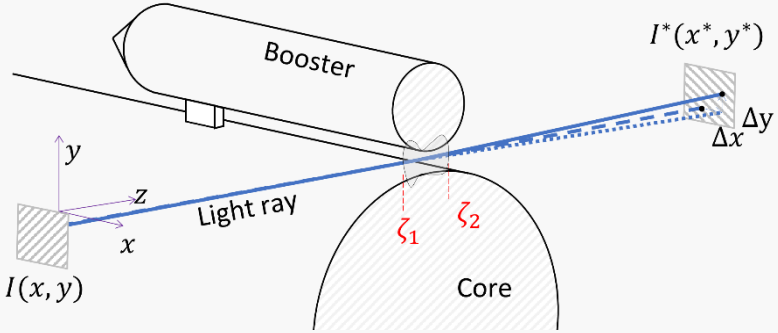


$$I^* = \sum I + \Delta I$$

[8]Panigrahi, P. K., and Muralidhar, K., "Schlieren and Shadowgraph Methods in Heat and Mass Transfer," SpringerBriefs in

Analytical considerations: simplifying assumptions

- Assumptions:
  - Linearizing $\ln n$ and applying Gladston-Dale formula
  - Ideal gas law, assuming:
    - Constant temperature (validated in more recent experiments)
    - Density variation is negligible everywhere along each path, s, except for the booster region between ζ_1 and ζ_2, or width L



$$\frac{\Delta I}{I} = lLK\left(\frac{\partial^2}{\partial x^2} + \frac{\partial^2}{\partial y^2}\right)P$$

Analytical considerations: periodic signal

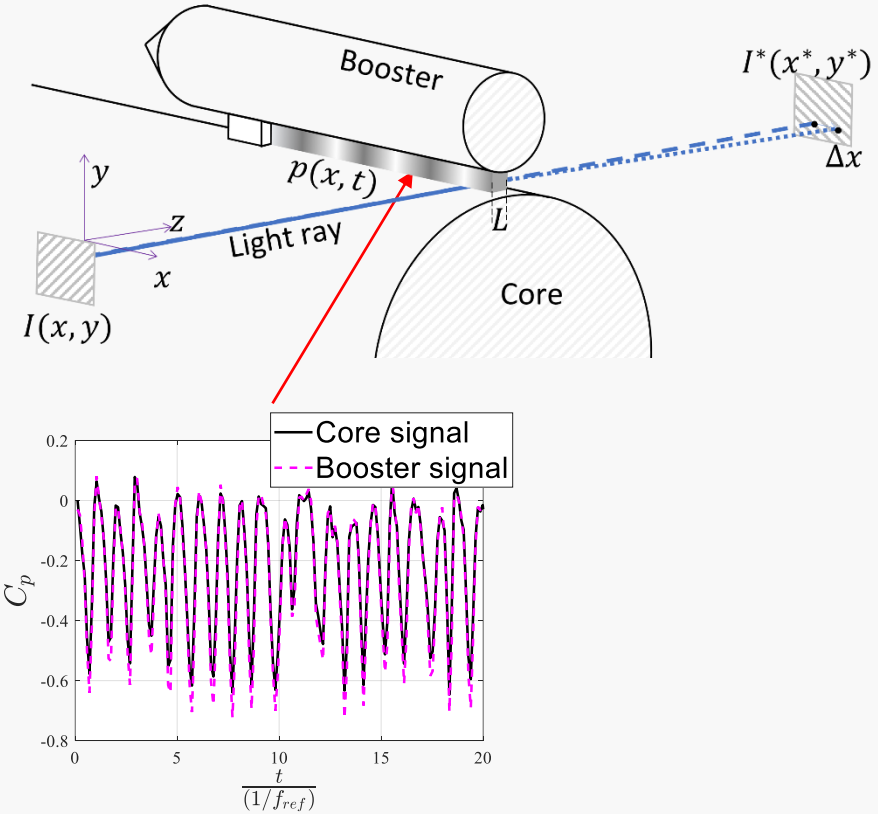
$$\frac{\Delta I}{I} = lLK\left(\frac{\partial^2}{\partial x^2} + \frac{\partial^2}{\partial y^2}\right)p$$

- Pressure signal, from the Kulite® transducers, downstream of the forward hardware attachment is periodic. So, p and $\frac{\Delta I}{I}$ can be expressed as sine functions:

$$p(x,t) = A_1 \sin(2\pi f_{x1} x + 2\pi f_1 t + \phi)$$

$$\frac{\Delta I}{I}(x,t) = A_2 \sin(2\pi f_{x2} x + 2\pi f_2 t + \phi)$$

- Assumed p is not a function of y, which is validated by nearly-identical signal observed in sensors on the booster and the core.



Analytical considerations: final equation form

$$\frac{A_2}{A_1} = lLK4\pi^2 f_{x1}^2$$

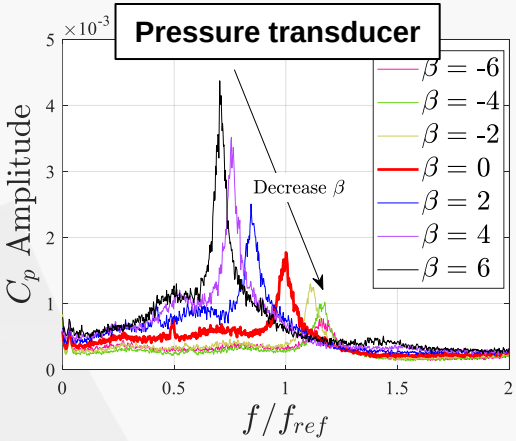
- Knowing the fluctuation amplitude of the pixel brightness and the pressure, a constant $C_1 = lLK4\pi^2$ can be solved by substitution in the above equation:

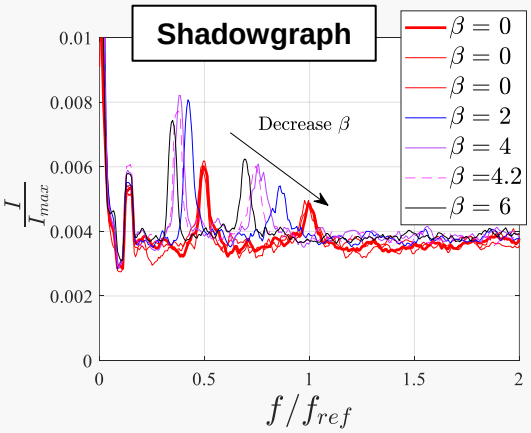
$$\frac{A_2}{A_1} = C_1 f_{x1}^2$$

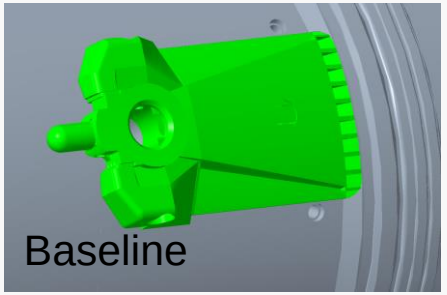
- Next step is to use the available shadowgraph and pressure data to find C_1

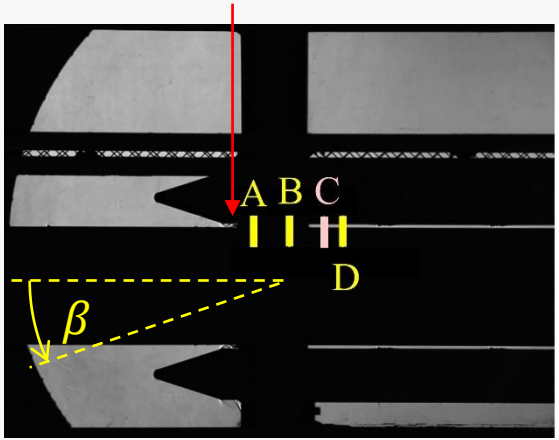
Results: β polar

- Sideslip, β, polar was used for the Baseline hardware attachment configuration to obtain C_1 calibration constant
- β polar provided a continuous variation of fluctuation amplitude, ideal for this calibration
- Pressure measurements at station C were used first





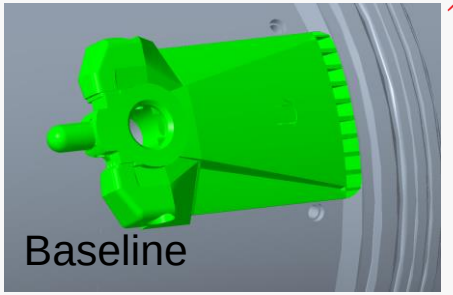


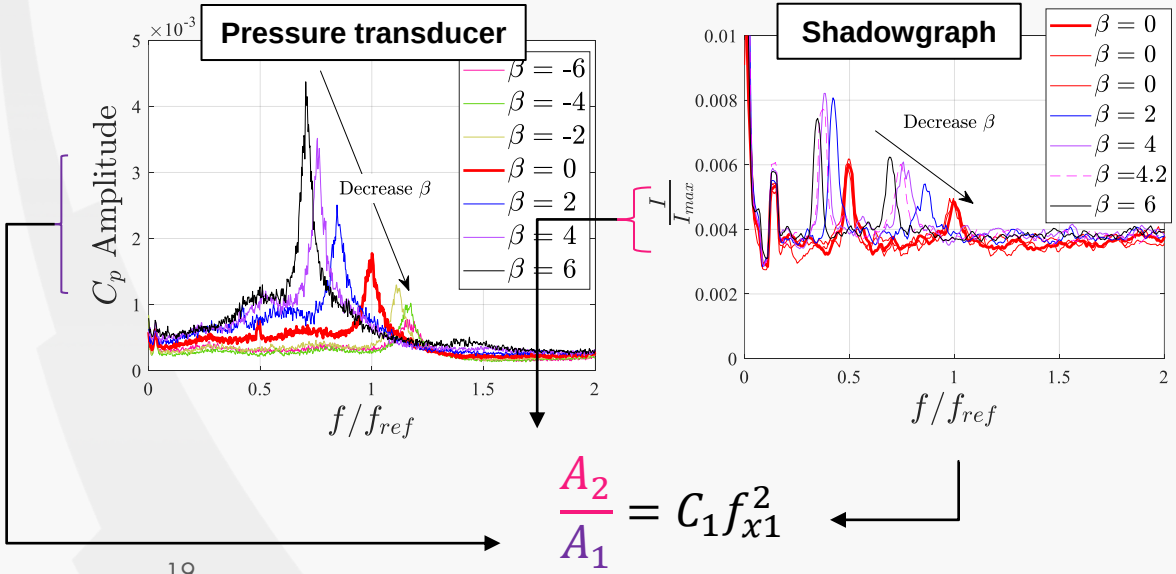


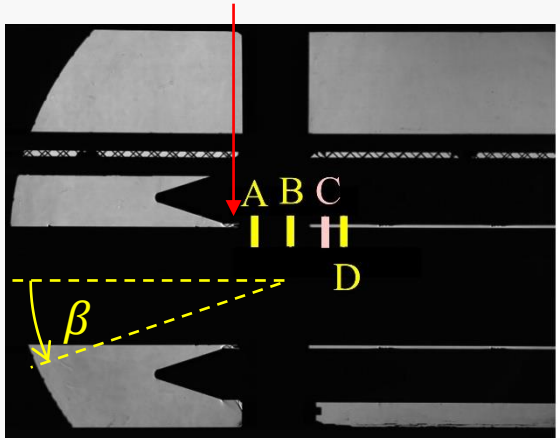
$$\frac{A_2}{A_1} = C_1 f_{x1}^2$$

Results: β polar

- For each β, a unique C_1 was computed
- $f_{x1} = f v_c$ where v_c is convective speed obtained from station-to-station cross correlation



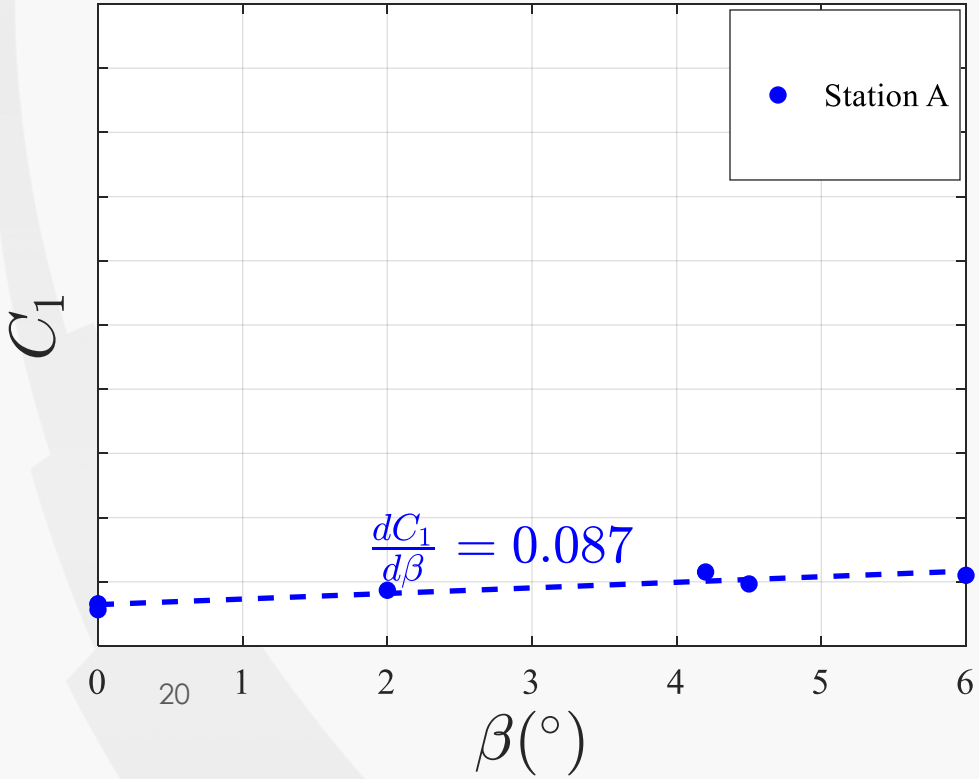


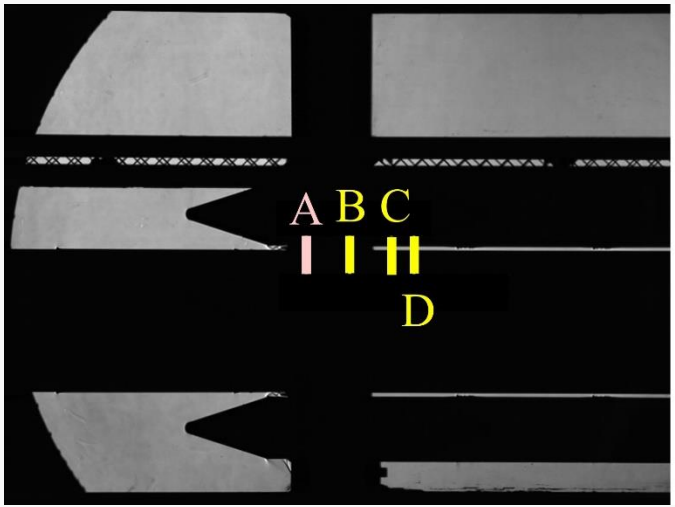


$$\frac{A_2}{A_1} = C_1 f_{x1}^2$$

Results: calibration constant

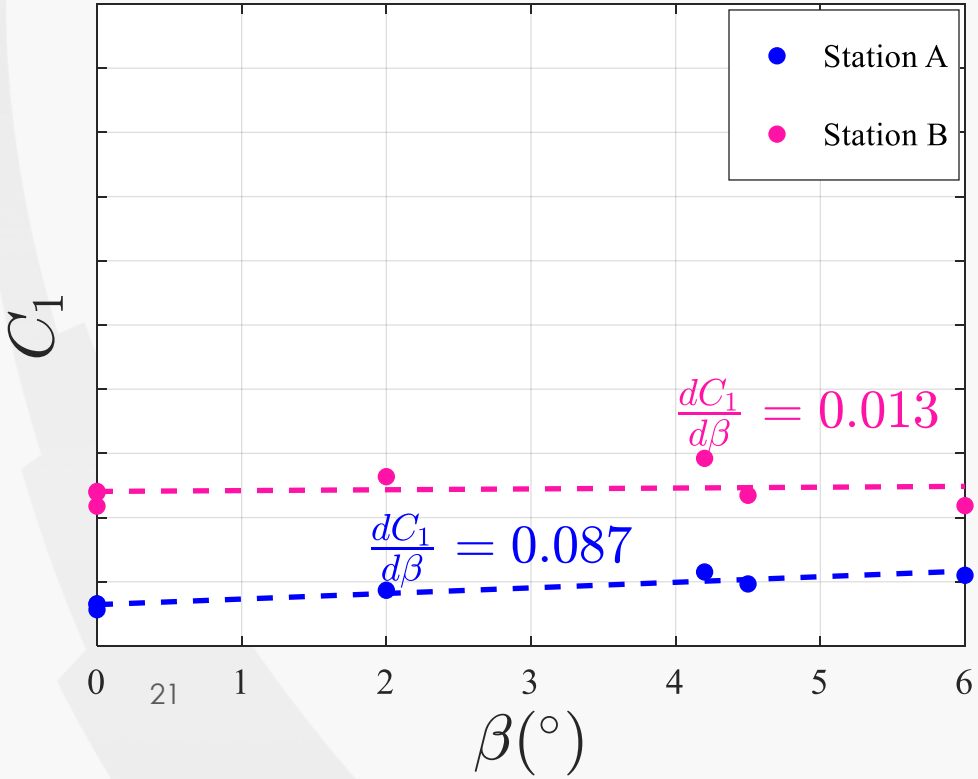
- C_1 for each β angle computed by comparing shadowgraph brightness intensity amplitude to measured pressure fluctuation amplitude at Station A

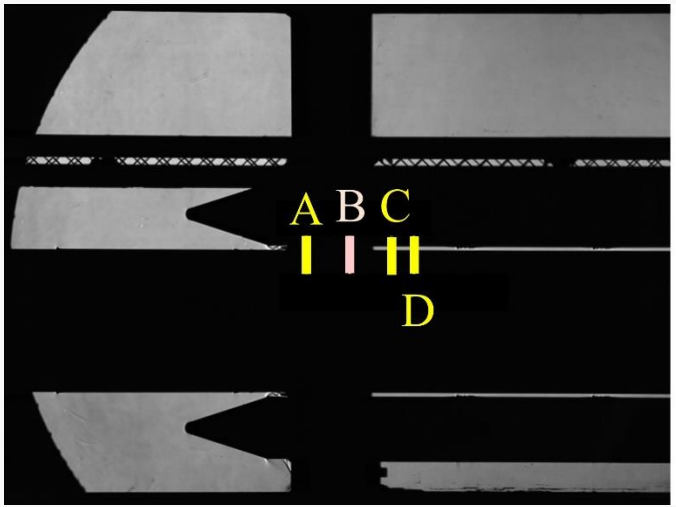




Results: calibration constant

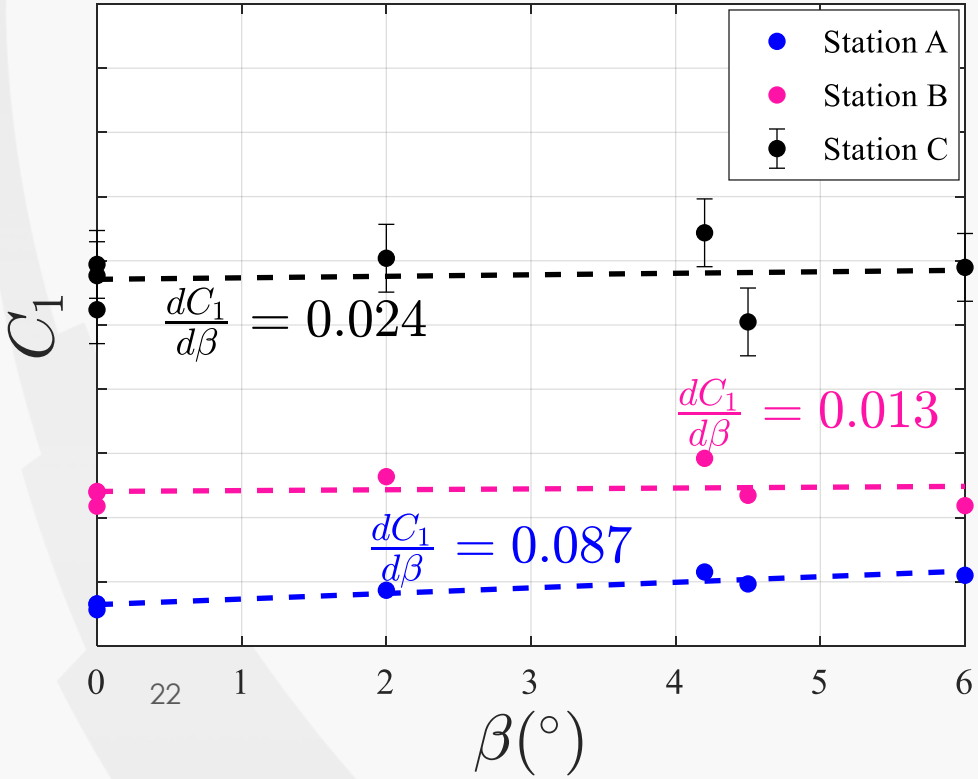
- C_1 for each β angle computed by comparing shadowgraph brightness intensity amplitude to measured pressure fluctuation amplitude at Station B

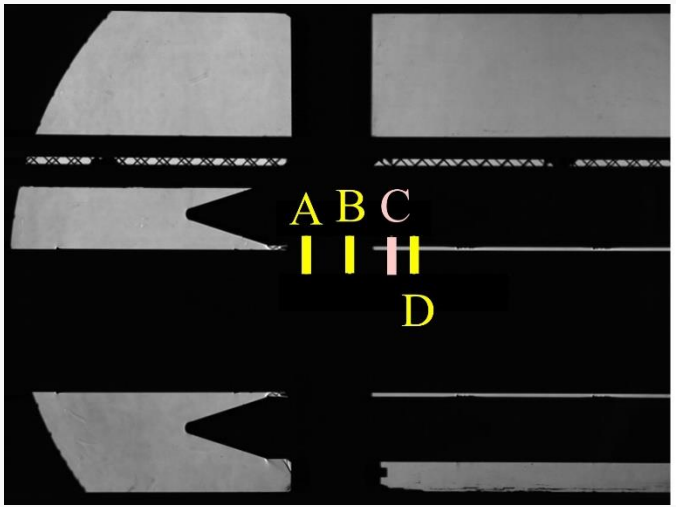




Results: calibration constant

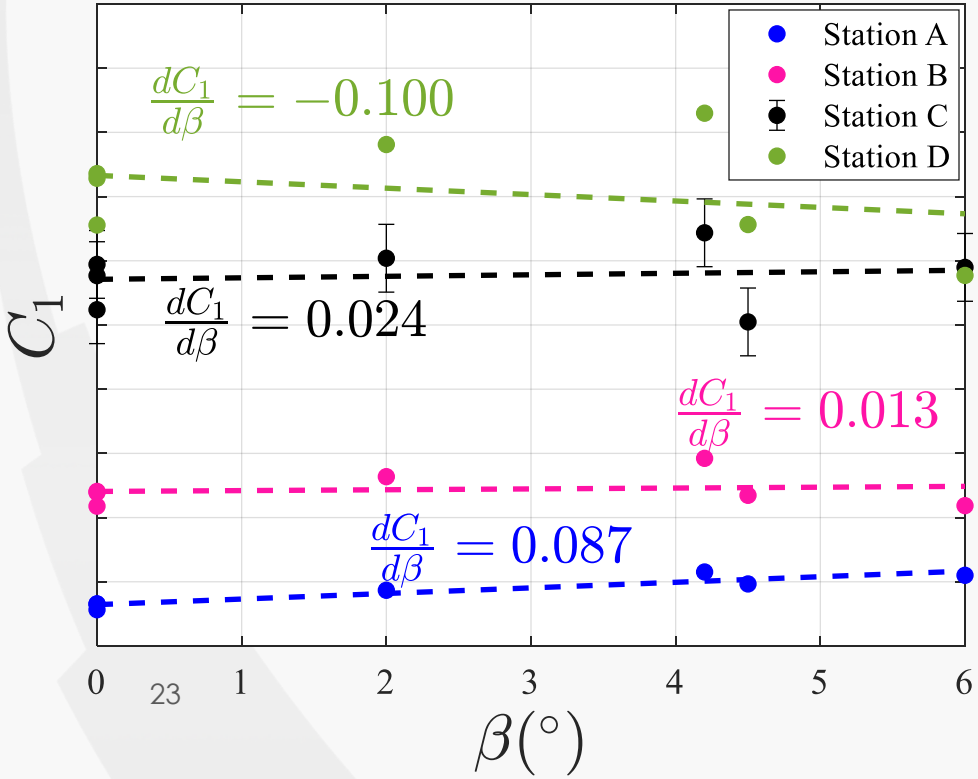
- C_1 for each β angle computed by comparing shadowgraph brightness intensity amplitude to measured pressure fluctuation amplitude at Station C

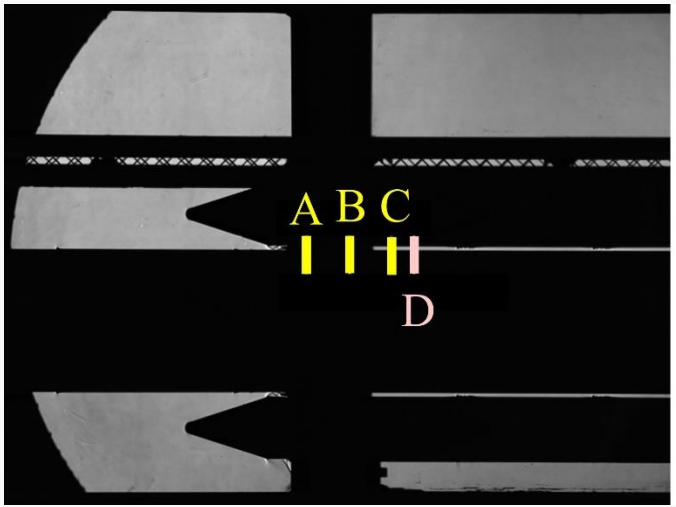




Results: calibration constant

- C_1 for each β angle computed by comparing shadowgraph brightness intensity amplitude to measured pressure fluctuation amplitude at Station D



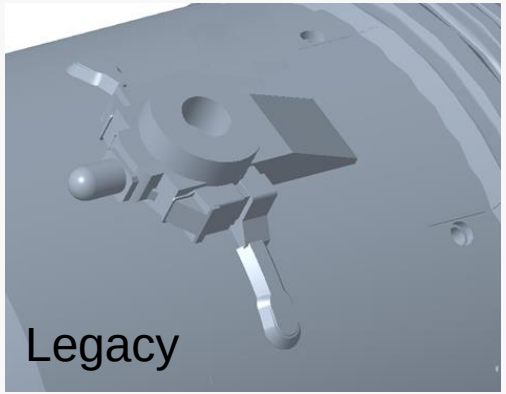


Results: calculation of pressure

- With known calibration coefficient C_1, shadowgraph-based pressure measurements can be obtained

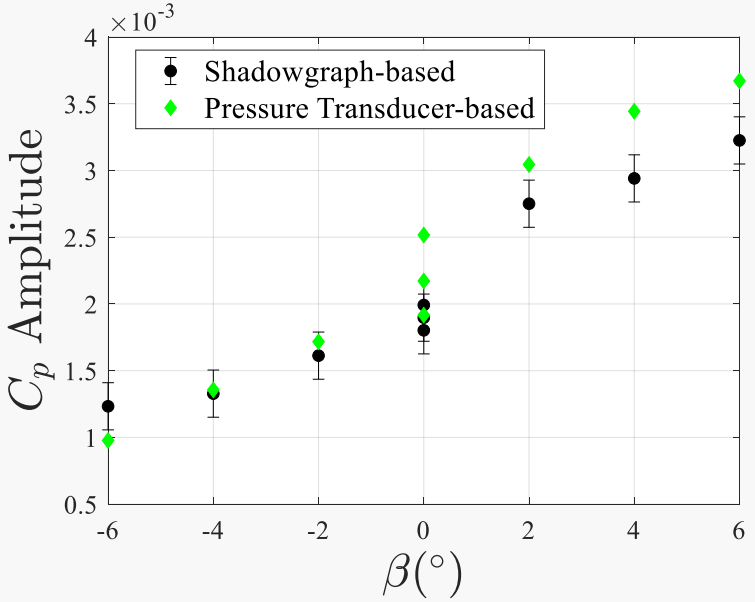
$$A_1 = \frac{A_2}{C_1 f_{x1}^2}$$

- Shadowgraph data for the Legacy hardware attachment test run was used to compute pressure fluctuations and compared them to the pressure transducer-based measurements.



Results: pressure fluctuation result

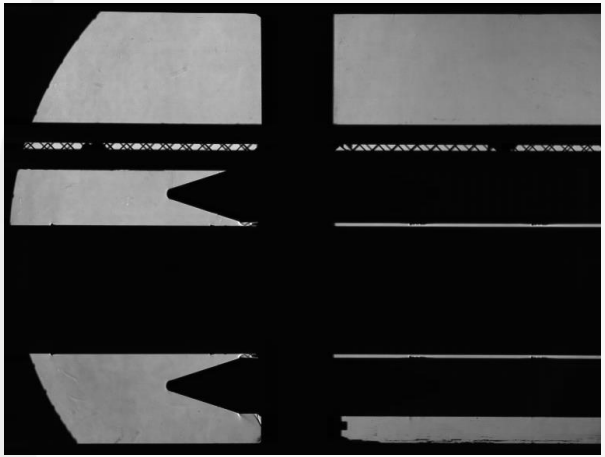
- Shadowgraph-based pressure measurements are within the experimental uncertainty for negative β values.
- Offset in measured pressure amplitude values is introduced stating at $\beta = 0$.
- This offset remains unexplained. Potential issue with excitation voltage.



Conclusions

- Quantitative flow visualization analysis was developed to **measure pressure fluctuations**
- The analysis required simplifications that were valid in the core-booster gap region
  - Constant-temperature
  - One-dimensional flow
  - Dominant fluctuations in density occur in the core-booster gap
- Calibration was performed using a **Baseline attachment** configuration of the wind-tunnel test
- The calibration constant was used to compute shadowgraph-based pressures and compare them to the pressure transducer-based measurements
- **Legacy attachment** configuration was used to verify the calibration constant
- Fluctuating pressure values were within experimental uncertainty for negative β angles

Questions?



Oleg Goushcha
Oleg.O.Goushcha@nasa.gov

